The Impact of Low-Level Cloud over the Eastern Subtropical Pacific on the "Double ITCZ" in LASG FGCM-0

DAI Fushan*[1,2] (戴福山), YU Rucong[1] (宇如聪), ZHANG Xuehong[1] (张学洪), YU Yongqiang[1] (俞永强), and LI Jianglong[1,3] (李江龙)

[1] *LASG, Institute of Atmospheric Physics, Chinese Academy of Sciences, Beijing* 100029

[2] *Beijing Institute of Applied Meteorology, Beijing* 100029

[3] *National Climate Center, Beijing* 100081

(Received April 22, 2002; revised March 4, 2003)

ABSTRACT

Like many other coupled models, the Flexible coupled General Circulation Model (FGCM-0) suffers from the spurious "Double ITCZ". In order to understand the "Double ITCZ" in FGCM-0, this study first examines the low-level cloud cover and the bulk stability of the low troposphere over the eastern subtropical Pacific simulated by the National Center for Atmospheric Research (NCAR) Community Climate Model version 3 (CCM3), which is the atmosphere component model of FGCM-0. It is found that the bulk stability of the low troposphere simulated by CCM3 is very consistent with the one derived from the National Center for Environmental Prediction (NCEP) reanalysis, but the simulated low-level cloud cover is much less than that derived from the International Satellite Cloud Climatology Project (ISCCP) D2 data. Based on the regression equations between the low-level cloud cover from the ISCCP data and the bulk stability of the low troposphere derived from the NCEP reanalysis, the parameterization scheme of low-level cloud in CCM3 is modified and used in sensitivity experiments to examine the impact of low-level cloud over the eastern subtropical Pacific on the spurious "Double ITCZ" in FGCM-0. Results show that the modified scheme causes the simulated low-level cloud cover to be improved locally over the cold oceans. Increasing the low-level cloud cover off Peru not only significantly alleviates the SST warm biases in the southeastern tropical Pacific, but also causes the equatorial cold tongue to be strengthened and to extend further west. Increasing the low-level cloud fraction off California effectively reduces the SST warm biases in ITCZ north of the equator. In order to examine the feedback between the SST and low-level cloud cover off Peru, one additional sensitivity experiment is performed in which the SST over the cold ocean off Peru is restored. It shows that decreasing the SST results in similar impacts over the wide regions from the southeastern tropical Pacific northwestwards to the western/central equatorial Pacific as increasing the low-level cloud cover does.

Key words: coupled model, double ITCZ, low-level cloud

1. Introduction

A double ITCZ (Inter-Tropical Convergence Zone) is a phenomenon featured with two ITCZs, one at each side of a the equator. Signatures of double ITCZ can possibly be found in all seasons over the western/central Pacific, but only during boreal spring, mainly in March and April, over the eastern Pacific (Zhang, 2001). So it is well known that the climate in the eastern tropical Pacific is asymmetrical about the equator with the ITCZ mostly north of the equator.

Unlike the fact that a double ITCZ exists only in boreal spring in the eastern Pacific, the phenomenon in most coupled models often persists all the year. This is one of the common deficiencies in most current coupled models. Mechoso et al. (1995) reviewed performances of 11 different coupled models. They found that the simulated equatorial cold tongue generally tends to be too strong, too narrow, and to extend too far west, SSTs are generally too warm in broad regions west of Peru, especially in a zonal band near 10°S, and this is

*E-mail: dfs@mail.iap.ac.cn

accompanied in 4 models by a double ITCZ straddling the equator over the eastern Pacific, and in 6 models by an ITCZ migrating across the equator with the seasons; only one model is accompanied by an ITCZ persisting north of the equator.

Philander et al. (1996) attributed the latitudinal climate asymmetry to two sets of factors: interactions between ocean and atmosphere that are capable of converting symmetry into asymmetry, and geometries of continents that determine the longitudes in which interactions are effective and the hemisphere in which the warmest water and the ITCZ are located. Since geometries of continents are realistic in the comprehensive coupled models, it is not because of an absence of realistic geometry that makes a symmetric climate over the eastern Pacific. The model symmetric climate feature such as the Double ITCZ may be attributed to reasons such as some important coupled feedbacks are absent or some coupled air-sea feedbacks are not properly treated. Mechoso et al. (1995) suggested that the specific mechanisms that may be associated with the failure to generate sufficient asymmetry in the coupled model include the evaporation-wind feedback and the effect of the stratus cloud.

Philander et al. (1996) found that only slightly asymmetric distribution of SSTs is simulated in the coupled model without the stratus parameterization, but the asymmetry over the eastern Pacific in the model would be significantly amplified with SSTs reduced in the southeastern Pacific when the stratus parameterization is introduced. Ma et al. (1996) studied results of an idealized sensitivity experiment in which a stratus cloud deck is prescribed to persist over the ocean off Peru (30°–10°S, 90°W–the Peruvian coast), and found that the prescribed stratus deck not only makes the SST beneath the stratus deck significantly reduced, but also largely alleviates the SST warm biases in the southeastern Pacific, producing a distribution of SSTs with more realistic inter-hemispheric asymmetries. Moreover, the prescribed stratus deck also makes the equatorial cold tongue unrealistically strong and extend too far west. Yu and Mechoso (1999) compared results of different sensitivity experiments in which the stratocumulus is prescribed to cover the ocean off Peru all year round, only in the first half of the year, and only in the second half of the year, respectively. They demonstrated that differences between the amplitude, duration, and westward propagation of the warm and the cold phases of the SST in the eastern equatorial Pacific are linked to the annual variations of the Peruvian stratocumulus, and only if the prescribed annual variations of Peruvian stratocumulus vary in phase with the observed variations are these differences successfully captured. Gordon et al. (2000) used the monthly mean low-level cloud fractions derived from the International Satellite Cloud Climatology Project (ISCCP) C2 data instead of the simulated fractions to study the sensitivity of the coupled model to the low-level cloud with more realistic annual variation. They demonstrated that the prescribed low-level cloud could make the distribution of SSTs over the eastern Pacific more asymmetric about the equator, the equatorial cold tongue intensified and farther westward, and the annual cycle of SSTs in the eastern equatorial Pacific strengthened. They also found that the ENSO-like inter-annual variability in the equatorial Pacific is apparently sensitivity to a 20% relative change of the low-level cloud fractions.

Like many other coupled models, the Flexible coupled ocean-atmosphere General Circulation Model (FGCM-0) of LASG, the State Key Laboratory of Numerical Modeling for Atmosphere Science and Geophysical Fluid Dynamics, also suffers from the spurious double ITCZ (Zhang et al., 2001**; Li, 2002). In order to understand the "Double ITCZ" in FGCM-0, this study will first examine the low-level cloud cover and the bulk stability of the low troposphere over the eastern subtropical Pacific in CCM3, which is the atmosphere component model of FGCM-0, and then sensitivity experiments will be performed to investigate whether and how the low-level cloud cover over the eastern subtropical Pacific impacts the double ITCZ in FGCM-0.

The model and the data used in this study are briefly described in section 2. Section 3 contains introductions and analyses of control experiments. Sensitive experiments are performed and analyzed in section 4. Some conclusions are summarized in section 5.

2. Model and data

FGCM-0 is being developed in LASG based on the NCAR Climate System Model version 1 (CSM-1) by replacing CSM-1's ocean component, NCOM, with the third generation global ocean general circulation model, L30T63, in IAP (Jin et al., 1999). Moreover, some necessary modifications are made to other component models of the CSM. The atmosphere and the land surface components are CCM3 (Kiehl et al., 1998) and LSM1 (Bonan, 1998), respectively.

The horizontal resolution of L30T63 is 1.875° × 1.875°. There are thirty layers in the vertical, of which

**Zhang, X., Y. Yu, J. Li, 2001: Towards understanding the 'double ITCZ' in a coupled ocean-atmosphere general circulation model, In ABSTRACT, IAMAS 2001, 10-18 July 2001, Innsbruck, Austria, S02.2-1-2, 19 (page 21).

twenty levels are placed within the upper 1000 m and twelve levels are placed in the upper 300 m to depict the equatorial thermocline better. Some fairly mature parameterizations are adapted to the model, including the penetration of solar radiation (Rosati and Miyakoda, 1988), the "PP" scheme for the upper ocean vertical mixing (Pacanowski and Philander, 1981), and the isopycnal mixing scheme "GP90" proposed by Gent and MacWilliams (1990). A thermodynamic sea-ice model based on Parkinson and Washington (1979) is also integrated into the ocean model. The model was first integrated for 1160 years from the static state with the wind stress forcing of Hellerman and Rosenstein (1983) and the thermal forcing required in a Haney-type formula for heat-flux (Haney, 1971), taken from the Comprehensive Ocean-Atmosphere Data Set, COADS (da Silva et al., 1994). The surface salinity in the model was simply relaxed to the climatological annual cycle of Levitus and Boyer (1994). At the end of the integration, the model reaches a quasi-equilibrium state, of which both the wind-driven circulation and the thermohaline circulation are reasonably simulated (Jin et al., 1999). This may be seen as the basic run of L30T63 that provides initial conditions for the coupled model. Since the geography of FGCM-0 is identical with that of L30T63, land-sea marks and surface types of CCM3 have been modified to match L30T63. The horizontal grid system of the sea ice model of Weatherly et al. (1998) has been modified to be the same as that in L30T63, too.

Component models communicate each other through the coupler. Functions of the flux coupler are: (1) controlling the time coordination of all component models of the climate system model; (2) calculating most of the interfacial fluxes; (3) communicating with component models for exchanging fluxes and some control parameters. The atmosphere, the land, and the sea ice component models communicate with the flux coupler every model hour, but the ocean model every model day. No flux correction is applied in the coupled model. For the details of the model see Yu et al. (2002).

The climate data used in this study include the monthly mean cloud fraction data from the ISCCP D2 data from 1984 through 1993 (Rossow and Schiffer, 1991; Rossow et al., 1996), the NCEP monthly mean temperature reanalysis from from 1984 through 1993 (Kalnay et al., 1996), and the thirty-year's monthly mean SSTs based on Shea et al. (1990).

3. Control experiments

3.1 *Introductions of control experiments*

In this study, three control experiments are performed, which are named CCM3-Exp, Spinup-Exp, and FGCM-Exp, respectively. CCM3-Exp is used to examine the capability of CCM3 to simulate the low-level cloud cover and the stability of the low troposphere, and to be compared with FGCM-Exp. Results of FGCM-Exp will be compared with those from sensitivity experiments performed in the following sections.

CCM3-Exp is the same as the "Run 1" in Yu et al. (2002), in which the atmosphere component model, CCM3, coupled with the land surface model, LSM1, is integrated for 5 years by using the observed climatological SSTs and sea-ice distribution based on Shea et al (1990). The daily state variables and radiation flux of the experiment at the lowest model level for the last four years are archived.

The ocean model, L30T63, coupled with the thermodynamic sea ice model of Weatherly et al. (1998), is integrated for seventy years from the 1160th year of its basic run. During the integration, surface wind stress and thermal forcing are taken from the archived daily state variables and radiation flux at the lowest model level for the last four years of "Run 1" in Yu et al. (2002). This seventy-year integration of the ocean model was referred to as "Run 2" in Yu et al. (2002). The Spinup-Exp in this study is the five-year integration of the ocean model continued from the "Run 2"

Following the "Run 2" step, the fully coupled model, FGCM-0, is integrated for five years with the initial conditions for atmosphere, land surface, ocean, and sea ice models taken from the end of "Run 1" and "Run 2" respectively. This five-year integration is referred to as FGCM-Exp here.

3.2 *The phenomenon of double ITCZ in FGCM-0*

The simulated annual mean SSTs based on the last three-year integration of FGCM-Exp and the observed annual mean SSTs derived from the monthly mean SSTs from 1950 through 1979 based on Shea et al. (1990) are shown in Fig. 1a and Fig. 1b, respectively. In Fig. 1a, the simulated SST is expressed by isotherms with a contour interval of 2°C; the surface wind is expressed by vectors with the vector scale shown at the bottom-left corner.

It is clear that the observed distribution of SSTs in the eastern Pacific is asymmetric relative to the equator with the 28°C isotherm west of 140°W. But, the simulated SSTs in FGCM-Exp are obviously warmer than the observed in the southeastern tropical Pacific, and the 28°C isotherm south of the equator extends eastward to about 110°W. Consequently, a warm SST band is formed nearby 10°S, which is parallel with the one north of the equator and makes the distribution of SSTs almost symmetric about the equator. Moreover,

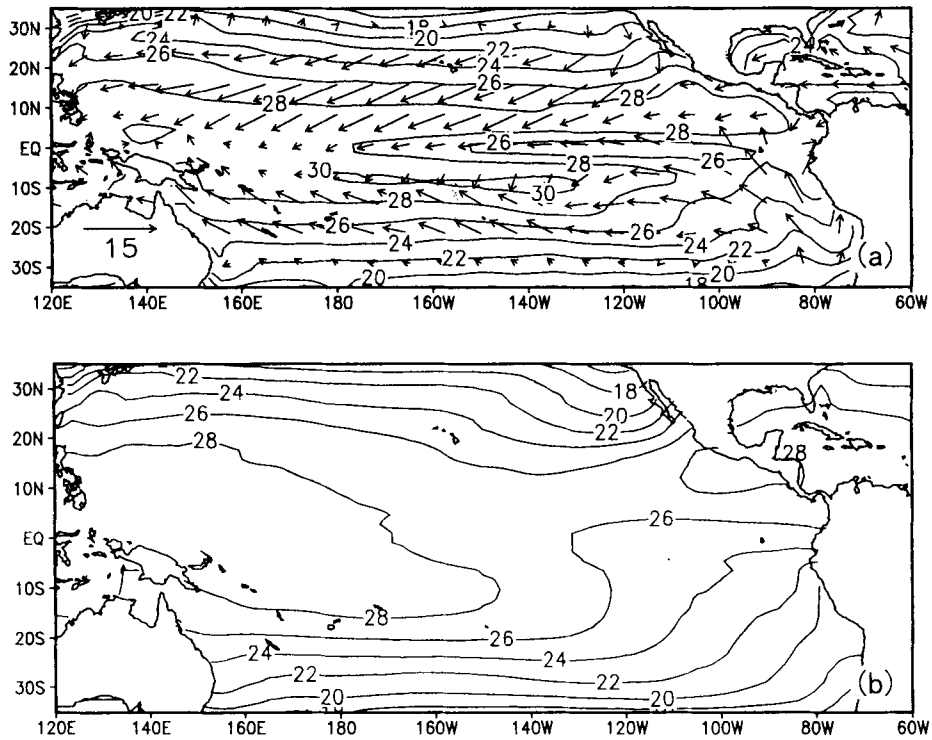

Fig. 1. (a) The simulated annual mean SST and surface wind in FGCM-Exp, (b) the observed annual mean SST. The contour interval of isotherms is 2°C. The simulated surface wind is expressed by vectors with the vector scale shown at the bottom-left corner in (a).

it is noticeable that the simulated equatorial clod tongue is strengthened and extends farther west. Accompanied with the convergence of the surface wind in the warm SST band, an ITCZ is formed south of the equator, which is parallel with the one north of the equator, and consequently a double ITCZ is formed (not shown here). So the feature of the symmetric distribution of SSTs in Fig. 1a is the reflection of the double ITCZ in FGCM-0.

3.3 *The low-level cloud cover and the stability of the low troposphere simulated by CCM3 and FGCM-0*

The observed and simulated annual mean low-level cloud cover are shown in Fig. 2a and Fig. 2b, respectively. Fig. 2a is derived from the monthly mean ISCCP data during 1984–1993. Fig. 2b is based on the last three-year integration of CCM3-Exp. The areas where the low-level cloud fraction is over 30% are shaded in Fig. 2a and Fig. 2b. It can be seen from Fig. 2 that, compared with the observed, the low-level cloud covers are markedly underestimated over the eastern subtropical Pacific, especially over the region off Peru and the region off California, but slightly overestimated over the eastern equatorial Pacific in CCM3-Exp.

In FGCM-Exp, in which the CCM3 is coupled with the ocean model L30T63, the low-level cloud covers simulated over the eastern subtropical Pacific are not only less than the observed, but also less than those simulated in the CCM3-Exp (not shown here).

Distributions of the annual mean bulk stability of the low troposphere derived from the NCEP temperature reanalysis and simulated by CCM3-Exp are shown in Fig. 3a and Fig. 3b, respectively. Here, the bulk stability is defined as the difference of potential temperature between 700 hPa and 1000 hPa. Figure 3a is derived from the NCEP monthly mean temperature reanalysis from 1984 through 1993, and Fig. 3b is obtained from the last three-year integration of CCM3-Exp. In Fig. 3, the contour interval is 2°C, and, the values greater than 14°C are shaded. It can be seen from Fig. 3 that the bulk stability of the low troposphere simulated by CCM3 is very consistent with that derived from the NCEP reanalysis, especially over the region off Peru and the region off California. But, the simulated stability is more intense than that derived from the NCEP data over the eastern equatorial Pacific south of the equator.

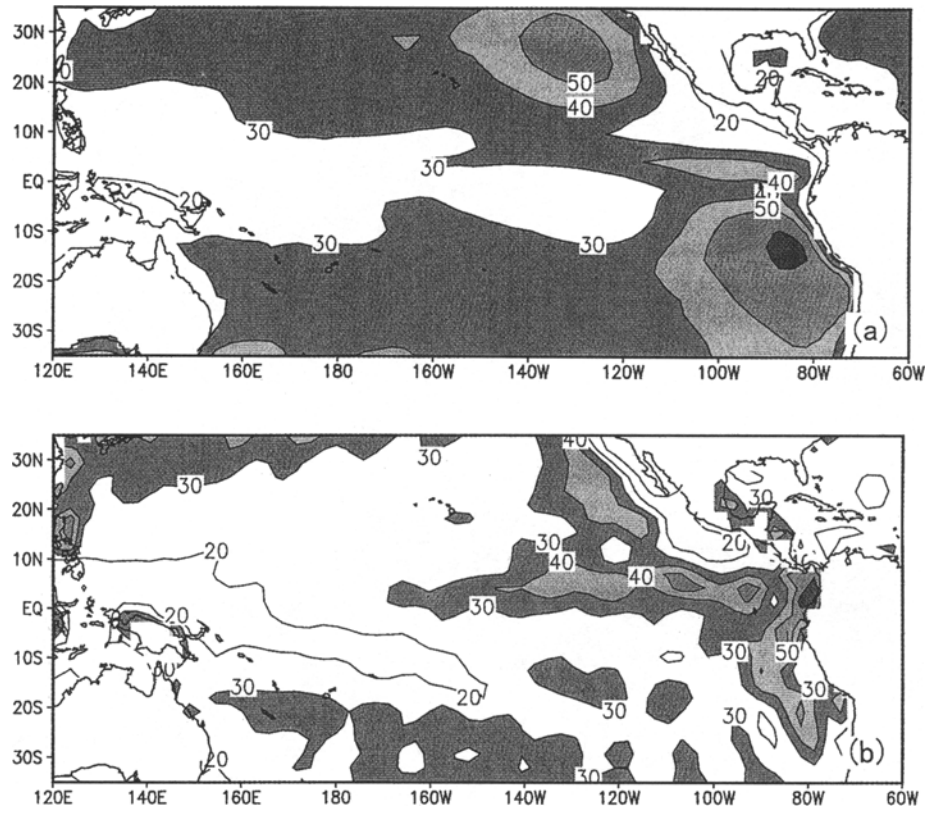

Fig. 2. The annual mean low-level cloud covers: (a) derived from ISCCP, (b) simulated by CCM3. Areas where the low-level cloud covers are over 30% are shaded.

In FGCM-Exp, the bulk stability of the low troposphere simulated over the eastern subtropical Pacific is also generally consistent with that derived from the NCEP reanalysis, but the strong stability center over the eastern equatorial Pacific extends farther west, and the one over the region off California extends farther west, too (not shown here).

3.4 *Discussions*

It is well known that the low-level stratus fraction is statistically correlated with the stability of the low troposphere over the marine stratus regions (Klein and Hartmann, 1993; Philander et al., 1996). Based on the ISCCP data and the NCEP reanalysis from 1984 through 1993, correlation coefficients between the low-level cloud cover and the bulk stability of the low troposphere are shown in Fig. 4. The bulk stability of the low troposphere is defined the same as in the previous subsection, and areas where the correlation coefficients are significant at the 99% level are shaded. It can be seen from Fig. 4 that there is a significant correlation between the low-level cloud cover and the bulk stability of the low troposphere over the eastern tropical and subtropical Pacific.

Slingo (1987) used the statistical relationship between the low-level stratus and the stability of the low troposphere, which was proposed from GATE data, to parameterize the subtropical low-level stratus in the ECMWF (European Center for Medium-Range Weather Forecasts) model. Slingo and Slingo (1991) introduced the scheme into the NCAR CCM. The scheme of low-level cloud in CCM3 is still based on Slingo (1987). According to Fig. 3 and Fig. 4, it seems that CCM3 should do a good job in simulating the low-level cloud cover over the eastern subtropical Pacific, but unfortunately it does very poorly as shown in Fig. 2b. This suggests that the parameterization scheme of the low-level cloud in CCM3 needs to be improved.

The low-level cloud over the eastern subtropical Pacific mainly consists of the low-level stratus (including stratocumulus). The underestimation of the low-level cloud cover over the eastern subtropical Pacific in CCM3 is due to its failure in simulating the low-level stratus. The scheme of the low-level stratus in CCM3 is based on the relative humidity and the maximum inversion strength defined by the difference of potential temperature between the two adjacent model levels, rather than based on the bulk stability of the low troposphere examined here. So the fact that CCM3 can successfully simulate the strong bulk stability centers but fails to simulate the low-level cloud cover centers

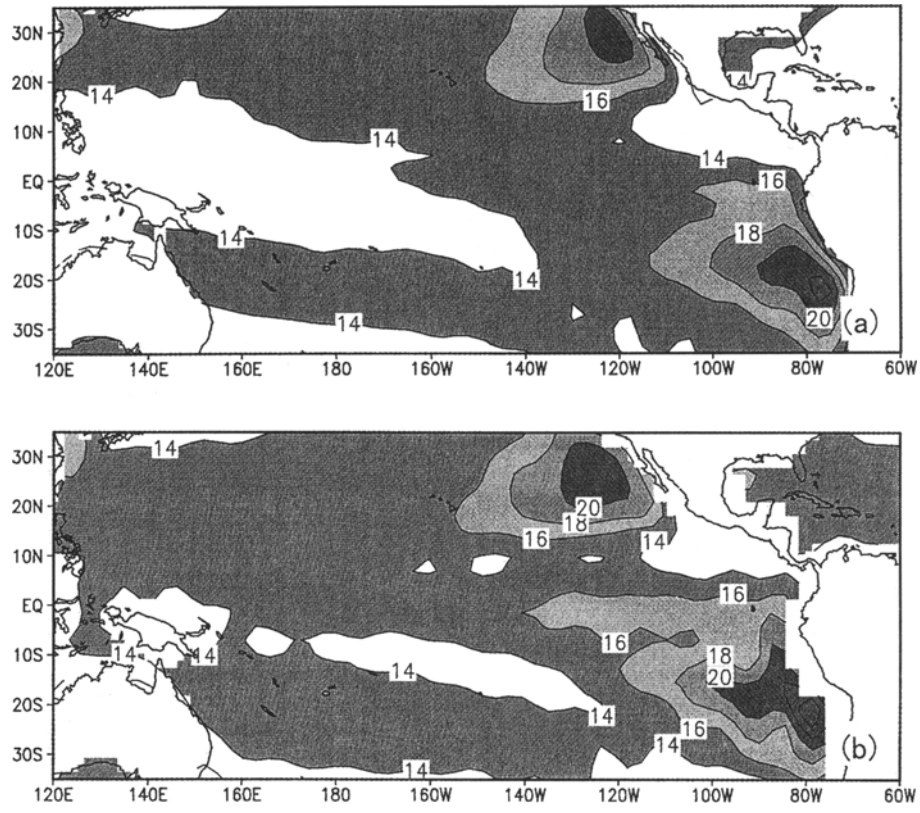

Fig. 3. The observed (a) and simulated (b) annual mean bulk stability of the low troposphere. The contour interval is 2°C. The values greater than 14°C are shaded.

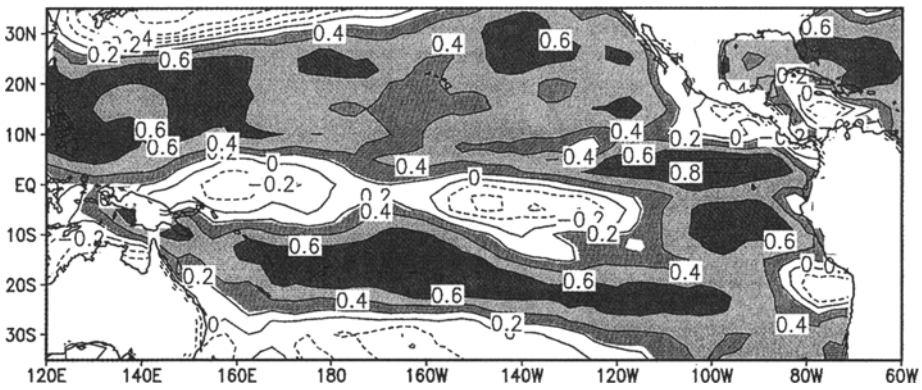

Fig. 4. The distribution of correlation coefficients between the low-level cloud cover and the bulk stability of the low troposphere based on the ISCCP data and the NCEP reanalysis from 1984 through 1993. The bulk stability is defined as the difference of potential temperature between 700 hPa and 1000 hPa. Areas where coefficients reach the 99% confidence level test are shaded. The contour interval is 0.2.

may be attributed to one or more of the following reasons. Firstly, CCM3 does not simulate well the maximum inversion strength at the top of the atmosphere boundary layer over some regions. Secondly, the base of the inversion simulated by CCM3 is higher than the observed so that the relative humidity at the base of the simulated inversion is too low to form the cloud (not shown here).

Based on the above, it can be seen that the formation of the double ITCZ in FGCM-0 is indeed associated with the fact that the low-level cloud covers over the eastern subtropical Pacific are underestimated by

the model's atmosphere component, CCM3.

4. Sensitivity experiments

4.1 *Designs of sensitivity experiments*

It has been demonstrated in the previous section that there is a strong correlation between the low-level cloud cover and the bulk stability of the low troposphere. Based on the aforementioned ISCCP data and the NCEP reanalysis from 1984 through 1993, over the region off the Peruvian coast (30°S–0°, 110°–80°W), a linear regressive equation between the low-level cloud cover and the bulk stability of the low troposphere is obtained as:

$$C_{\text{low}} = 0.0503839(\theta_{700} - \theta_{1000}) - 0.383777\,, \quad (1)$$

where C_{low} is the low-level cloud cover, θ_{700} is the potential temperature at 700 hPa, and θ_{1000} is the potential temperature at 1000 hPa. The correlation coefficient in Eq.(1) is 0.77.

Similarly, over the region off California (10°–35°N, 150°– 120°W), a linear regressive equation between the low-level cloud cover and the bulk stability of the low troposphere is obtained as:

$$C_{\text{low}} = 0.0343625(\theta_{700} - \theta_{1000}) - 0.1472345\,, \quad (2)$$

where, $C_{\text{low}}, \theta_{700}$, and θ_{1000} are the same as in Eq.(1). The correlation coefficient in equation (2) is 0.76.

In order to understand the impacts of the low-level cloud covers over the eastern subtropical Pacific on the double ITCZ in FGCM-0, two sensitivity experiments named CldSen1 and CldSen2, respectively, are performed based on the model FGCM-0.

CldSen1 is almost the same as FGCM-Exp except that the scheme of the low-level cloud in CCM3 over the region of 20°S–0°, 110°–80°W, is replaced by Eq.(1), and the cloud cover calculated by Eq.(1) is placed on the immediate model level just above the top of the planetary boundary layer.

Similarly, CldSen2 is almost the same as FGCM-Exp except that the schemes of the low-level cloud in CCM3 over the region of 30°–5°S, 110°–80°W off Peru and that over the region of 10°–35°N, 150°–120°W off California are replaced by the Eq.(1) and (2), respectively. The cloud cover calculated by Eq.(1) or Eq.(2) is also placed on the immediate model level just above the top of the planetary boundary layer.

Moreover, in order to understand the feedback between the SST and the low-level cloud cover over the region off Peru, another sensitivity experiment named SstSen is performed. SstSen is almost the same as FGCM-Exp except that SSTs simulated by the model in the area of 20°S–0°, 110°–80°W, are restored to those SSTs from Spinup-Exp by the following equation:

$$\begin{aligned}\frac{\partial T}{\partial t} = & -V_{\text{h}} \cdot \nabla T - w\frac{\partial T}{\partial z} + A_{\text{hh}} \triangle T \\ & + \frac{\partial}{\partial z}\left(A_{\text{hv}}\frac{\partial T}{\partial z}\right) + \frac{1}{\rho c_p}\frac{\partial F_A}{\partial z} + \mu(T_{\text{s}} - T)\,,\end{aligned} \quad (3)$$

where T is the water temperature in the model, T_{s} is the water temperature output from the Spinup-Exp, t is the model time, V_{h} is the horizontal velocity, w is the vertical velocity, z is the depth of water, A_{hh} is the horizontal diffusion coefficient, A_{hv} is the vertical diffusion coefficient, ρ is sea water density, c_p is the specific heat of water, F_A is vertical heat flux, μ is the time coefficient, and μ is taken as $1/(20$ days), which means that the e-folding time scale is 20 days. The left hand side of Eq.(3) is temperature tendency. On the right-hand side of Eq.(3), the first and second terms are horizontal and vertical advections, the third and fourth terms are horizontal and vertical diffusions, the fifth is the heat flux term, and the sixth is the restoring term added by the experiment.

4.2 *Analyses of results of CldSen1 experiment*

Since CldSen1 is almost the same as FGCM-Exp except that a new scheme of the low-level cloud is used locally over the region off Peru, differences between results of CldSen1 and those of FGCM-Exp directly reflect impacts of the low-level cloud off Peru on the performance of the FGCM-0.

Compared with results of FGCM-Exp, the low-level cloud covers over the region off Peru are markedly increased in CldSen1 as shown in Fig. 5. The figure shows differences of the simulated annual mean low-level cloud covers between CldSen1 and FGCM-Exp. The contour interval is 10% and positive values are shaded. Low-level cloud covers over the western equatorial Pacific and over the ITCZ north of the equator are also increased in CldSen1. But, medium and high cloud covers over regions from the Peruvian coast to the western equatorial Pacific are significantly decreased in CldSen1. Consequently, total cloud covers are increased over the region off Peru, but decreased over the western/central equatorial Pacific (not shown here).

With the increase of low-level cloud covers over the region off Peru in CldSen1, the net solar heat flux reaching the surface is locally decreased. But with the

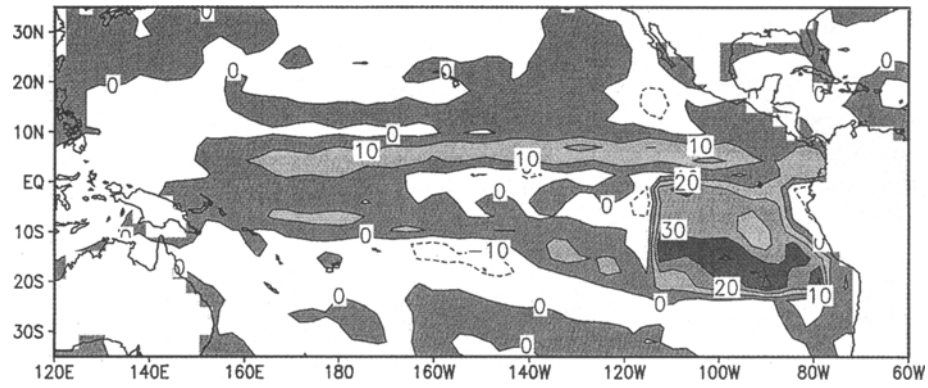

Fig. 5. Differences of the simulated annual mean low-level cloud covers between CldSen1 and FGCM-Exp. Contour interval is 10%, and positive values are shaded.

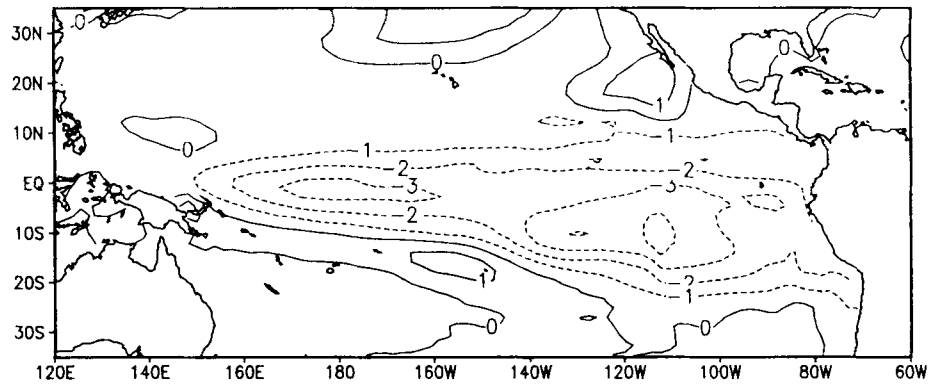

Fig. 6. Differences of the simulated annual mean SSTs between CldSen1 and FGCM-Exp. Contour interval is 1°C. Negative values are expressed by dashed lines.

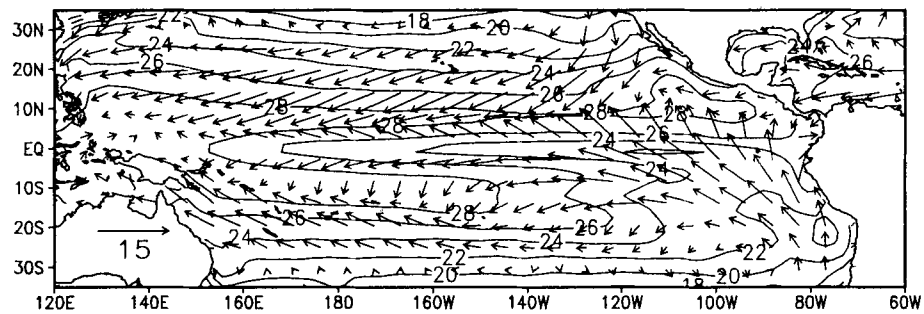

Fig. 7. The annual mean SSTs and surface wind simulated by CldSen1. The SST is expressed by isotherms with contour interval 2°C. The surface wind is expressed by vectors with the vector scale at the bottom-left corner.

the decrease of total cloud covers, mainly attributed to the decrease of high cloud covers, the net solar heat flux reaching the surface is increased over the western/central equatorial Pacific (not shown here). Accompanied with the reduction of net solar heat flux reaching the surface, SSTs over the region off Peru are obviously decreased as shown in Fig. 6. The figure shows differences of the simulated annual mean SSTs between CldSen1 and FGCM-Exp. The contour interval is 1°C and negative values are expressed by dashed

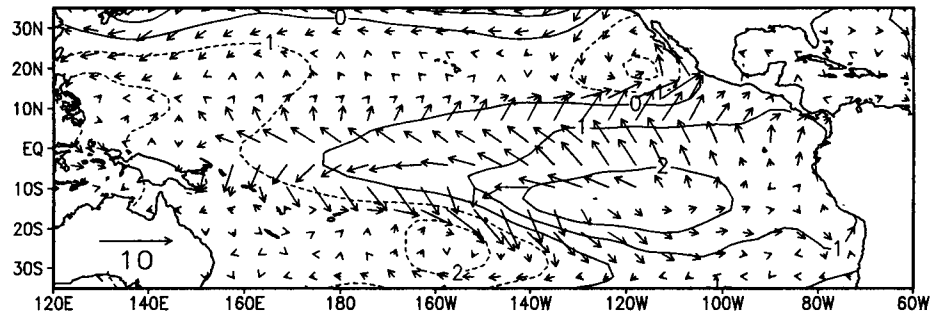

Fig. 8. Differences of the simulated sea level pressure and surface wind between CldSen1 and FGCM-Exp. The difference of sea level pressure is expressed by isobars with contour interval 1 hPa and the difference of surface wind is expressed by vectors with the vector scale at the bottom-left corner.

lines.

In Fig. 6, it is clear that the increase of low-level cloud cover off Peru makes SSTs decrease not only over the local region off Peru, but also over wide regions from the Peruvian coast northwestwards to the western/central equatorial Pacific. The marked decrease of SST in the southeastern tropical Pacific effectively restrains the warm SST band south of the equator from extending too far east. Accompanied with the westward retreat of the warm SST band south of the equator, the convergence zone of the surface wind near 10°S also retreats westward (see Fig. 7 and Fig. 1a). Consequently, the spurious ITCZ south of equator is, to some extent, suppressed. But the remarkable decrease of SST over the western/central equatorial Pacific makes the equatorial cold tongue extend too far west as shown in Fig. 7. The figure shows the annual mean SST and the surface wind simulated by CldSen1. SSTs are expressed by isotherms with a contour interval of 2°C and the surface wind is expressed by vectors with the vector scale shown at the bottom-left corner.

Figure 8 shows differences of the simulated sea level pressure and surface wind between CldSen1 and FGCM-Exp. The difference of sea level pressure is expressed by isobars with a contour interval of 1 hPa and the difference of surface wind is expressed by vectors with the vector scale shown at the bottom-left corner. It can be seen that, compared with the results of FGCM-Exp, sea level pressure becomes higher and the surface southeast wind becomes stronger over regions where SSTs are much decreased in CldSen1.

The strengthened surface wind over the western/central equatorial Pacific and southeastern Pacific would result in a strong cooling effect on SSTs, and hence would significantly decrease SSTs over there. By recalling the fact that the net solar heat fluxes reaching the surface simulated by CldSen1 are enhanced over these areas, it can be said that the remarkable decrease of SST over the western/central equatorial Pacific and eastern tropical Pacific south of the equator in CldSen1 is mainly due to the cooling processes associated with the strengthened southeast wind. However, it is noticeable in Fig. 8 that the difference of surface southeast wind between CldSen1 and FGCM-Exp is very small over the region off Peru, but the net solar heat fluxes reaching the surface simulated by CldSen1 are much reduced over there. So it can be concluded that the decrease of SST over the region off Peru is mainly due to the reduced net solar heat fluxes reaching the surface rather than the cooling effect associated with the southeast wind.

4.3 *Analyses of results of CldSen2 experiment*

Results of the CldSen2 experiment are very similar to those of CldSen1. Compared with results of FGCM-Exp, low-level cloud covers are increased both over the region off Peru and over the region off California, but medium and high cloud covers are decreased over wide regions from the Peruvian coast northwestwards to the western equatorial Pacific, and consequently, total cloud covers are increased off Peru and off California, but decreased over the western/central equatorial Pacific. This results in the reduction of the net solar heat fluxes reaching the surface off Peru and off California, but an increase over the western/central equatorial Pacific. With the increase of low-level cloud covers over the region off Peru, sea level pressure becomes higher, surface southeast wind is strengthened, and SSTs are decreased over wide regions from the Peruvian coast northwestwards to the western equatorial Pacific (not shown here). Consequently, the warm SST band south of the equator is effectively hindered from extending too far east as shown in Fig. 9. The figure shows the

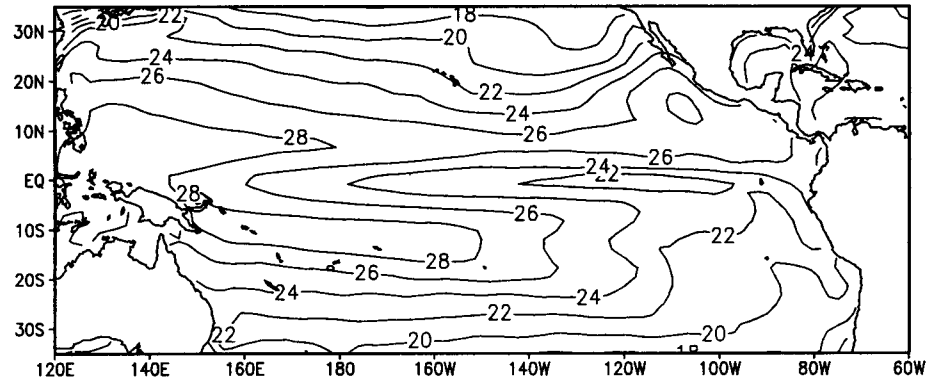

Fig. 9. The annual mean SST simulated by CldSen2. Contour interval is 2°C.

annual mean SSTs derived from the last three-year integration of CldSen2 in which the contour interval is 2°C.

Comparing Fig. 9 with Fig. 7 shows that the warm SST biases in the ITCZ north of the equator are reduced with the isotherm of 28°C broken over the central/eastern tropical Pacific, and hence producing a more realistic distribution of SSTs north of the equator in the tropical Pacific. This is obviously the result of the increase of low-level cloud cover over the region off California. It can also be seen that the equatorial cold tongue becomes more intense and extends farther west in CldSen2 than in CldSen1. The possible mechanism which makes the equatorial cold tongue extend westward will be discussed in section 4.5.

4.4 *Analyses of results of SstSen experiment*

Results of the SstSen experiment are also very similar to those of CldSen1. In SstSen, corresponding to the decrease of SST in the region off Peru as a result of being restored to those from Spinup-Exp, low-level cloud covers are increased off Peru, but medium and high cloud covers are decreased over regions from the Peruvian coast northwestwards to the western equatorial Pacific, and consequently, total cloud covers are increased over the region off Peru, but decreased over the western/central equatorial Pacific. This results in the reduction of the net solar heat fluxes reaching the surface over the region off Peru, but an increase over the western/central equatorial Pacific. With the decrease of SSTs in the local region off Peru, SstSen makes sea level pressure become higher, surface southeast wind strengthen, and SSTs decrease over wide regions from the Peruvian coast northwestwards to the western equatorial Pacific (not shown here). The warm SST band south of the equator is also hindered from extending too far east in SstSen like that in CldSen1, as shown in Fig. 10. The figure shows the annual mean SSTs derived from the last three-year integration of SstSen in which the contour interval is 2°C. But it can be seen from the figure that the equatorial cold tongue is weaker and does not extend as far west in SstSen as the one in CldSen1.

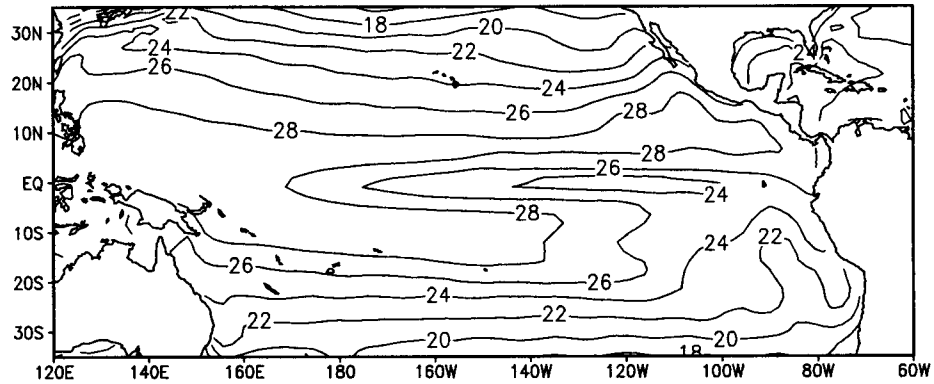

Fig. 10. The annual mean SSTs simulated by SstSen. Contour interval is 2°C.

4.5 *Discussions*

It has been seen that low-level cloud covers over the eastern subtropical Pacific were underestimated by CCM3, but were reasonably simulated over the local region off Peru in CldSen1 and both over the local region off Peru and over the local region off California in CldSen2. A new scheme of low-level cloud, which is only dependent on the regressive relation between the low-level cloud cover and the bulk stability of the low troposphere, is used in CldSen1 and CldSen2 instead of the original scheme in CCM3. The original scheme in CCM3 is not only based on the maximum inversion strength, which is defined by the difference of potential temperatures between the two adjacent model levels, but also based on the relative humidity. So differences of the simulated low-level cloud covers between CldSen1 (CldSen2) and CCM3-Exp might be attributed to the following reasons. Firstly, though the bulk stability of the low troposphere is well simulated by CCM3, the maximum stability at the top of the planetary boundary layer may not be well simulated. Secondly, the simulated temperature field may be mismatched with the simulated relative humidity field so that the relative humidity at the base of the inversion may be too low to form cloud in CCM3.

Based on the aforementioned analyses, it can be seen that with the increase of low-level cloud cover over the eastern subtropical Pacific, the double ITCZ in FGCM-0 is, to some extent, suppressed. Increasing the low-level cloud off California can reduce the warm SST biases in the ITCZ north of the equator and hence produce a more realistic distribution of SSTs over the tropical Pacific north of the equator. Increasing the low-level cloud cover over the region off Peru can reduce the warm SST biases in the southeastern tropical Pacific, and hence effectively hinder the warm SST band south of the equator from extending too far east, but it can also make the equatorial cold tongue become much more intensified and extend too far west.

SstSen further demonstrates that there is a positive feedback between the SST and the low-level cloud cover over the region off Peru. Either decreasing the SST or increasing the low-level cloud cover over the region off Peru will make sea level pressure increase, surface southeastern wind strengthen, and SSTs decrease not only over the local region off Peru, but also over wide regions from the Peruvian coast northwestwards to the western/central equatorial Pacific. The mechanism involved may be concluded as shown in Fig. 11.

With an increase of low-level cloud covers over the region off Peru, the net solar heat fluxes reaching the surface will be reduced, and hence SSTs will be decreased over the local region. The decrease of the SST will be favorable for strengthening the stability of the low troposphere and the low-level inversion, which will be more conducive to increasing the low-level cloud cover, and therefore a thermodynamic positive feed-

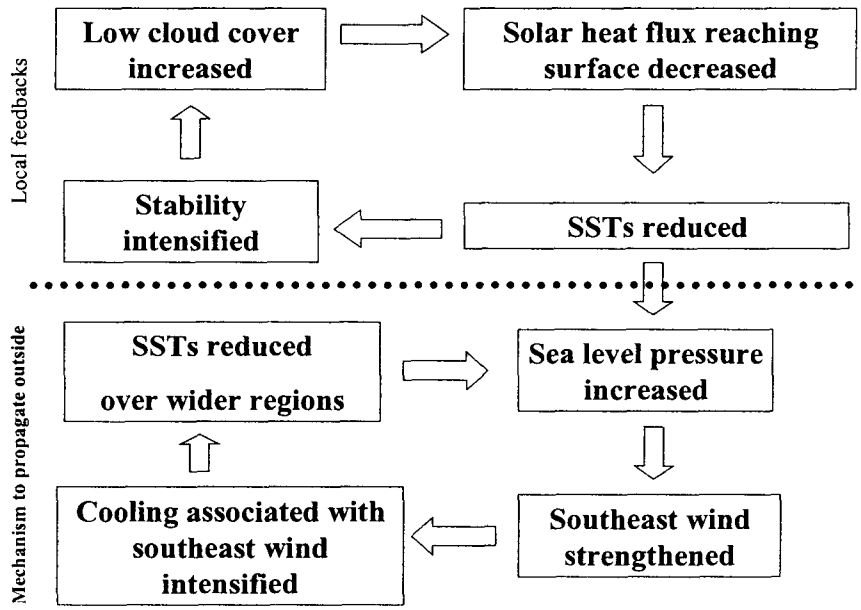

Fig. 11. The sketch map of the mechanisms involving impacts of low-level cloud covers over the region off Peru.

back involving the SST and the low-level cloud will be formed locally. On the other hand, the decrease of the SST will increase sea level pressure and strengthen surface southeast wind, which will intensify the latitudinal Hadley circulation and zonal Walker circulation (Yu and Mechoso, 1999). With the surface wind strengthened, the associated cooling effect will also be intensified, and therefore SSTs will be decreased over much wider regions. This will further enhance sea level pressure over much wider regions, and consequently a dynamical mechanism will be formed, which will make the local impacts of low-level cloud over the region off Peru propagate northwestwards.

Liu and Xie's (1994) theoretical analysis demonstrates that an extratropical annual forcing along the coast of South America can effectively influence the equatorial cold tongue through equatorward and westward propagation of the coupled disturbances by wind-evaporation-entrainment feedback. Ma et al. (1996) suggested that the cooling immediately to the west and north of the region with the prescribed stratus deck is primarily associated with the increased evaporation as the southeast trade wind is strengthened, and that the cooling along the equator in the central Pacific is mainly due to the enhanced oceanic cold advection. Processes involved in the equatorward and westward propagation mechanism are not analyzed here and need to be studied further.

The aforementioned mechanism can be used to partly interpret why the double ITCZ is formed in the FGCM-0. The less low-level cloud cover over the region off Peru simulated by the atmosphere component model, CCM3, will cause the net solar heat fluxes reaching the surface to be overestimated, and hence will cause the SST to be increased locally. The increase of SST, on one hand, will degrade the stability of the low troposphere, which will go against the formation of the low-level cloud cover. On the other hand, it will lower sea level pressure. The lowered sea level pressure will cause the surface southeast wind and the associated cooling effect to be weakened, which will result in the warm SST biases over wider regions. Accompanied with the convergence of surface wind in the warm SST band near 10°S, a spurious ITCZ will appear south of the equator, and hence a double ITCZ will be formed in FGCM-0. Moreover, the underestimation of low-level cloud cover over the region off California makes the SST in ITCZ north of the equator too warm.

It should be noted that the underestimation of low-level cloud cover over the region off Peru is not the sole factor that causes the formation of the double ITCZ in FGCM-0. Solely increasing the low-level cloud cover will not thoroughly eliminate the double ITCZ in the model, but to the contrary, it will also make the equatorial cold tongue become more intense and extend farther west. The possible mechanism may be concluded as follows. With the increase of the low-level cloud cover over the region off Peru, surface southeast wind will become more intensive. This will cause the upwelling and cooling effects to be strengthened over the eastern equatorial Pacific, which will make the SST further decrease and hence make the equatorial cold tongue intensify. Moreover, the decrease of the SST will cause sea level pressure to become high and the stability of the low troposphere to be strengthened. The enhanced sea level pressure will strengthen the east wind in the equatorial Pacific. This will make the upwelling and the cooling effect propagate westward in the equatorial Pacific, and therefore will make the equatorial cold tongue extend westward. Why the simulated equatorial cold tongue is stronger and extends farther west than the observed one needs to be studied in the future.

Liu (2001) found no signal of a double ITCZ over the eastern tropical Pacific when he directly coupled the atmospheric general circulation model used in the National Climate Center, China, with L30T63. After examining the cloud cover simulated by his coupled model, it was found that his coupled model could reasonably simulate the two centers of the low-level cloud over the region off Peru and off California, respectively (not shown here). So, it can be seen that it is important to properly describe the low-level cloud cover over the eastern subtropical Pacific for improving the performance of the coupled model.

5. Conclusions

Based on the aforementioned analyses and discussions, the following conclusions are obtained.

The bulk stability of the low troposphere simulated by CCM3 is very consistent with the one derived from the NCEP reanalysis, but the low-level cloud covers simulated by CCM3 are significantly underestimated over the eastern subtropical Pacific. This suggests that the parameterization scheme of the low-level cloud in CCM3 needs to be improved.

The underestimation of the low-level cloud cover over the region off Peru in CCM3 is one of the main factors that result in the warm SST biases in the eastern tropical Pacific, and hence the formation of the double ITCZ in FGCM-0. Increasing the low-level cloud cover over the region can effectively reduce the warm SST biases in the southeastern Pacific, and hence, to some extent, suppress the double ITCZ in FGCM-0. But, on the other hand, it can also make the equatorial cold tongue become much more intensified and extend

farther west. So, the underestimation of the low-level cloud cover over the region off Peru in CCM3 is not the sole factor that causes the formation of the double ITCZ in FGCM-0.

The underestimation of low-level cloud cover over the region off California in CCM3 is one of the factors which result in the warm SST biases in the ITCZ north of the equator in FGCM-0. Increasing the low-level cloud cover over the region can effectively reduce the warm SST biases in the tropical Pacific north of the equator.

There is a positive feedback between the SST and the low-level cloud cover over the region off Peru. Increasing the low-level cloud cover over the region off Peru will result in similar effects over wide regions from the Peruvian coast to the western/central equatorial Pacific as decreasing the SST over the region off Peru will do.

It may be through processes associated with the southeast wind that make impacts of low-level cloud covers or SSTs over the region off Peru propagate northwestwards from the southeastern Pacific to the western/central equatorial Pacific.

Acknowledgments. The authors would like to thank Dr. Liu Hailong and Dr. Li Wei for their assistance in processing data. Dr. Liu Xiyong helped the authors to examine the cloud covers simulated by his coupled model and provided valuable comments. We also appreciate useful comments from two anonymous reviewers. This study was jointly supported by the National Natural Science Foundation of China under Grant No.40023001 and No. 40233031 and "Innovation Program" under Grant ZKCX2–SW–210, and the National Key Basic Research Project under Grant G200078502.

REFERENCES

Bonan, G. B., 1998: The land surface climatology of the NCAR land surface model coupled to the NCAR community climate model. *J. Climate*, **11**, 1307–1326.

da Silva, A. M., C. C. Young, and S. Levitus, 1994: *Atlas of Surface Marine Data 1994, Vol.1: Algorithms and Procedures*, NOAA Atlas NECDIS 6, U. S. Dept. of Commerce, Washington D. C., 83pp.

Gent, P. R., and J. C. McWilliams, 1990: Isopycnal mixing in ocean circulation models. *J. Phys. Oceanogr.*, **20**, 150–155.

Gordon, C. T., A. Rosati, and R. Gudgel, 2000: Tropical sensitivity of a coupled model to specified ISCCP low clouds. *J. Climate*, **13**, 2239–2260.

Haney, R. L., 1971: Surface thermal boundary condition for ocean circulation models. *J. Phys. Oceanogr.*, **1**, 241–248.

Hellerman, S., and M. Rosenstein, 1983: Normal monthly wind stress data over the world ocean with error estimates. *J. Phys. Oceanogr.*, **13**, 1093–1104.

Jin Xiangze, Zhang Xuehong, and Zhou Tianjun, 1999: Fundamental framework and experiments of the third generation of IAP/LASG world ocean general circulation model. *Advances in Atmospheric Sciences*, **16**(2), 197–215.

Kalnay, E., and Coauthors, 1996: The NCEP/NCAR 40-year reanalysis project. *Bull. Amer. Meteor. Soc.*, **77**, 437–471.

Kiehl, J. F., J. J. Hack, G. B. Bonan, B. A. Boville, D. L. Williamson, and P. J. Pasch, 1998: The National Center for Atmospheric Research community climate model: CCM3. *J. Climate*, **11**, 1131–1149.

Klein, S. A., and D. L. Hartmann, 1993: The seasonal cycle of low stratiform clouds. *J. Climate*, **6**, 1587–1606.

Levitus, S., and T. P. Boyer, 1994: *World Ocean Atlas 1994 Volume 3: Salinity*, NOAA Atlas NESDIS3. U. S. Department of Commerce, Washington, D. C., 99pp.

Li Jianglong, 2002: Analysis of double ITCZ phenomena in a coupled ocean-atmosphere general circulation model. M. S. thesis, Institute of Atmospheric Physics, Chinese Academy of Sciences, 65pp. (in Chinese)

Liu, Z., and S.-P. Xie, 1994: Equatorward propagation of coupled air-sea disturbances with application to the annual cycle of the eastern tropical Pacific. *J. Atmos. Sci.*, **51**, 3807–3822.

Liu Xiyong, 2001: The simulation and study of sea-ice-air interaction in the northern high latitude region. Ph.D. dissertation, Institute of Atmospheric Physics, Chinese Academy of Sciences, 136pp. (in Chinese)

Ma, C. C., Carlos R. Mechoso, Andrew W. Robertson, and Akio Arakawa, 1996: Peruvian stratus clouds and the tropical Pacific circulation: A coupled ocean-atmosphere GCM study. *J. Climate*, **9**, 1635–1645.

Mechoso, C. R., and Coauthors, 1995: The seasonal cycle over the tropical Pacific in coupled ocean-atmosphere general circulation models. *Mon. Wea. Rev.*, **123**, 2825–2838.

Pacanowski, R. C., and G. Philander, 1981: Parameterization of vertical mixing in numerical models of the tropical ocean. *J. Phys. Oceanogr.*, **11**, 1442–1451.

Parkinson, C. L., and W. M. Washington, 1979: A large-scale numerical model of sea ice. *J. Geophys. Res.*, **84**, 311–337.

Philander, S. G. H., D. Gu, D. Halpern, G. Lambert, N. C. Lau, T. Li, and R. C. Pacanowski, 1996: Why the ITCZ is mostly north of the equator. *J. Climate*, **9**, 2958–2972.

Rosati, A., and K. Miyakoda, 1988: A general circulation model for upper ocean circulation. *J. Phys. Oceanogr.*, **18**, 1601–1626.

Rossow, W. B., and R. A. Schiffer, 1991: ISCCP cloud data products. *Bull. Amer. Meteor. Soc.*, **72**, 2–20.

Rossow, W. B., A. W. Walker, D. E. Beuschel, and M. D. Roiter, 1996: International Satellite Cloud Climatology Project (ISCCP) documentation of new cloud datasets. WMO/TD-No.737, World Meteorological Organization, Geneva, Switzerland, 115pp.

Shea, D. J., K. E. Trenberth, and R. W. Reynolds, 1990: A global monthly mean sea surface temperature climatology. NCAR Tech. Note NCAR/TN-345, 167pp.

Slingo, J. M., 1987: The development and verification of a cloud prediction scheme for the ECMWF model. *Quart. J. Roy. Meteor. Soc.*, **113**, 899–927.

Slingo, A., and J. M. Slingo, 1991: Response of the National Center for Atmospheric Research community climate model to improvements in the representation of clouds. *J. Geophys. Res.*, **96**, 15341–15357.

Weatherly, J. W., B. P. Briegleb, W. G. Large, and J. A. Maslanik, 1998: Sea ice and polar climate in the NCAR CSM. *J. Climate*, **11**, 1472–1486.

Yu, J.-Y., and C. R. Mechoso, 1999: Links between annual variations of Peruvian stratocumulus clouds and of SST in the eastern equatorial Pacific. *J. Climate*, **12**, 3305–3318.

Yu Yongqiang, Yu Rucong, Zhang Xuehong, and Liu Hailong, 2002: A flexible coupled ocean-atmosphere general circulation model. *Advances in Atmospheric Sciences*, **19**(1), 169–190.

Zhang Chidong, 2001: Double ITCZs. *J. Geophys. Res.*, **106**, 11785–11792.

副热带东太平洋低云对LASG耦合环流模式FGCM–0 中“双ITCZ” 的影响

戴福山　宇如聪　张学洪　俞永强　李江龙

摘　要

与其他耦合环流模式一样，LASG耦合模式FGCM-0也存在虚假的“双ITCZ”。为了认识FGCM-0中“双ITCZ”，首先研究了FGCM-0的大气分量模式，即NCAR（美国国家大气研究中心）的公用气候模式CCM3对秘鲁和加利福尼亚沿岸低云以及低层大气整体稳定度的模拟能力。发现：尽管CCM3模拟的低层大气整体稳定度与利用NCEP（美国国家环境预报中心）再分析资料分析的结果较一致，但模拟的低云量比ISCCP（国际卫星云气候计划）观测值显著偏少。利用ISCCP低云量与由NCEP再分析温度场分析的低层整体稳定度之间的回归关系，修改了CCM3中低云参数化方案，并用于敏感性试验，以研究副热带东太平洋低云对FGCM-0中“双ITCZ”的影响。结果发现，修改的方案能显著增强对低云量的模拟，秘鲁沿岸冷海域低云量增加能显著减弱赤道以南热带东太平洋海表面温度（SST）的暖偏差，但同时也将使赤道冷舌增强、向西伸展更远；加利福尼亚沿岸低云量增加可以有效减弱赤道以北ITCZ区SST暖偏差。为了检验秘鲁沿岸SST与低云间的正反馈，又实施了一个控制秘鲁沿岸SST的敏感性试验，结果表明：控制秘鲁沿岸SST抑制其增暖，对自东南太平洋向西北至中、西赤道太平洋广大区域产生的影响，与增加秘鲁沿岸低云量产生的影响相似。

关键词：耦合模式，“双ITCZ”，低云